Functional Specialization of Maize Mitochondrial Aldehyde Dehydrogenases[1]

Feng Liu and Patrick S. Schnable*

Departments of Zoology and Genetics (F.L., P.S.S.) and Agronomy (P.S.S.), Interdepartmental Genetics Program (F.L., P.S.S.), and Center for Plant Genomics (P.S.S.), Iowa State University, Ames, Iowa 50011

The maize (*Zea mays*) *rf2a* and *rf2b* genes both encode homotetrameric aldehyde dehydrogenases (ALDHs). The RF2A protein was shown previously to accumulate in the mitochondria. In vitro import experiments and ALDH assays on mitochondrial extracts from *rf2a* mutant plants established that the RF2B protein also accumulates in the mitochondria. RNA gel-blot analyses and immunohistolocation experiments revealed that these two proteins have only partially redundant expression patterns in organs and cell types. For example, RF2A, but not RF2B, accumulates to high levels in the tapetal cells of anthers. Kinetic analyses established that RF2A and RF2B have quite different substrate specificities; although RF2A can oxidize a broad range of aldehydes, including aliphatic aldehydes and aromatic aldehydes, RF2B can oxidize only short-chain aliphatic aldehydes. These two enzymes also have different pH optima and responses to changes in substrate concentration. In addition, RF2A, but not RF2B or any other natural ALDHs, exhibits positive cooperativity. These functional specializations may explain why many species have two mitochondrial ALDHs. This study provides data that serve as a basis for identifying the physiological pathway by which the *rf2a* gene participates in normal anther development and the restoration of Texas cytoplasm-based male sterility. For example, the observations that Texas cytoplasm anthers do not accumulate elevated levels of reactive oxygen species or lipid peroxidation and the kinetic features of RF2A make it unlikely that *rf2a* restores fertility by preventing premature programmed cell death.

Aldehyde dehydrogenases (ALDHs) oxidize aldehydes to the corresponding carboxylic acid and simultaneously reduce NAD^+ and/or $NADP^+$. Over 300 ALDH genes have been identified from mammals, insects, bacteria, yeast, and plants (Sophos et al., 2001). The nomenclature of the ALDH super gene family was recently revised taking into account the evolutionary distances among the proteins encoded by these genes (Sophos et al., 2001). Family 1 ALDHs include the original Class 1 ALDHs, which are targeted to the cytosol. Family 2 consists of the Class 2 ALDHs, which are targeted to the mitochondria. In mammals and yeast, at least one role of Family 1 and 2 ALDHs is the detoxification of ethanol-derived acetaldehyde (Wang et al., 1998). Family 3 ALDHs of mammals are involved in the detoxification of aldehydes that form during lipid peroxidation (Lindahl and Petersen, 1991). Some of the Family 3 ALDHs are, in addition, expressed in tumors (Satomichi et al., 2000), where they are thought to be involved in antitumor drug resistance (Sladek, 1988). Other roles of ALDHs include vitamin A biosynthesis (Hind et al., 2002) and amino acid metabolism (Davies, 1959; Styrvold et al., 1986; Ferrandez et al., 1997). In bacteria, ALDHs are, in addition, involved in the metabolism of rare sugars (Boronat et al., 1983). In insects, ALDHs are involved in both the detoxification of aldehydes and the biosynthesis of pheromones (Morse and Meighen, 1984).

Although ALDHs of many species have been well characterized (Perozich et al., 1999), until recently little research had been performed on plant ALDHs. This began to change after it was established that the maize (*Zea mays*) *rf2a* gene encodes a mitochondrial ALDH that accumulates in the mitochondrial matrix (Cui et al., 1996; Liu et al., 2001). The *rf2a* gene, which was previously designated *rf2*, was originally defined by its ability, in conjunction with another nuclear gene, *rf1*, to restore fertility to Texas cytoplasmic male sterility (cmsT) maize lines (for review, see Laughnan and Gabay-Laughnan, 1983). Cytoplasmic male sterility (cms) has been observed in over 140 plant species (Schnable and Wise, 1998) and is an important agricultural trait used to facilitate the production of hybrid seed. Recently, it has been established that *rf2a* is involved not only in restoring male fertility to cmsT plants, but also plays an important role in anther development in plants that carry normal cytoplasm. Specifically, the anthers in the lower florets of normal cytoplasm plants that are homozygous for mutants in *rf2a* undergo developmental arrest (Liu et al., 2001).

The identification of these important developmental roles for an ALDH has stimulated additional re-

search on this relatively poorly studied class of plant enzymes. Since the time when *rf2a* was cloned, many additional plant ALDH genes have been cloned. For example, two ALDH genes have been isolated from tobacco (*Nicotiana tabacum*; op den Camp and Kuhlemeier, 1997), three from Arabidopsis (Skibbe et al., 2002), three from rice (*Oryza sativa*; Nakazono et al., 2000; Li et al., 2000), two from sorghum (*Sorghum bicolor*; GenBank accession nos. AB084897 and AB084898), and one from barley (*Hordeum vulgare*; Meguro et al., 2001). In addition, three additional ALDH genes have been cloned from maize (Skibbe et al., 2002).

Like all other plant species characterized to date, the maize genome contains two mtALDH genes, *rf2a* and *rf2b*, which encode proteins termed RF2A and RF2B (or according to the nomenclature of Sophos et al. [2001], ALDH2B1 and ALDH2B6). The RF2B protein exhibits 78.7% amino acid identity and 83.4% similarity with RF2A (Skibbe et al., 2002). To date, only very limited kinetic analyses have been conducted on plant mtALDHs and those that have been reported were performed using only partially purified protein preparations (Davies, 1959; Asker and Davies, 1985). Therefore, these studies could not distinguish the specific characteristics of the distinct mtALDHs. To understand the specific physiological roles of these enzymes, it is necessary to separately characterize the kinetic properties of the two mtALDHs from a single species.

In tobacco, ALDH-dependent ethanolic fermentation occurs during pollen development and growing pollen tubes even under aerobic conditions (Tadege and Kuhlemeier, 1997; Mellema et al., 2002). This pathway is thought to provide additional energy for pollen development and pollen tube growth. It has been established previously that both RF2A and RF2B can oxidize acetaldehyde (Liu et al., 2001; Skibbe et al., 2002). Although these findings are consistent with a role for RF2A in ethanolic fermentation, T cytoplasm-induced male sterility is associated with the premature degeneration of the tapetal layer of anthers. Although the accumulation of RF2A is enhanced in tapetal cells (Liu et al., 2001), it is not known whether ethanolic fermentation occurs in these cells. Of further concern is the observation that mammalian and yeast mtALDHs can oxidize a broad range of aldehydes. The identification of the specific pathway in which the *rf2a*-encoded mtALDH functions during fertility restoration and anther development will be complicated if, like mammalian and yeast mtALDHs, maize mtALDHs are capable of oxidizing many aldehydes.

In this study, the kinetic properties of purified recombinant RF2A and RF2B were determined and compared. These analyses reveal that the two maize mtALDH have very different substrate preferences and other kinetic properties, thereby suggesting that they have functionally distinct physiological roles.

RESULTS

RF2A and RF2B Accumulate in Mitochondria

The algorithm pSORT (http://psort.nibb.ac.jp/; Nakai and Kanehisa, 1992) predicted that RF2A (previously designated RF2) contains the mitochondrial targeting motif QRFST (amino acid index numbers 48–52, GenBank accession no. U43082). It has been established recently that the RF2A protein accumulates in the mitochondrial matrix (Liu et al., 2001). To determine the cleavage site of RF2A's mitochondrial targeting sequence, the N-terminal sequence of the mature RF2A protein was determined. RF2A was partially purified via immunoprecipitation from mitochondria isolated from etiolated seedlings of the N cytoplasm version of the inbred line Ky21. The partially purified protein was subjected to SDS-PAGE and then transferred to a polyvinylidene difluoride (PVDF) membrane. The protein band was excised and subjected to N-terminal sequencing. This analysis revealed that the cleavage site is between Phe-50 and Ser-51 (data not shown), which indicates that Arg-49 is located at the −2 position and Ser-51 at the +1 position. This result is in agreement with the predicted cleavage motif R − x*[A/S] − [T/S] (where an asterisk indicates the cleavage site; Sjöling and Glaser, 1998).

The algorithm pSORT predicted that the RF2B protein is also targeted to the mitochondria. Its predicted mitochondrial-targeting sequence is HRFST (amino acid index numbers 46–50, GenBank accession no. AF348417), which fits both the R-2 and R-3 models of Sjöling and Glaser (1998). To determine whether the RF2B protein is targeted to the mitochondria, RF2B protein was labeled with ^{35}S-Met via in vitro transcription and translation. The labeled protein was then incubated with freshly isolated maize mitochondria. The mitochondria were purified again after the in vitro import procedure and incubated with proteinase K in the presence or absence of Triton X-100 and/or valinomycin. After these incubations, the proteins extracted from the mitochondrial preparations were analyzed via SDS-PAGE.

After incubation of RF2B protein with mitochondria, a novel protein that is smaller than RF2B accumulates (Fig. 1). Proteins that are attached to the exterior of mitochondria, but that have not been imported, are susceptible to proteinase K digestion in the absence of Triton X-100. Although the RF2B precursor protein is susceptible to proteinase K digestion, in the absence of Triton X-100 the novel protein is resistant to proteinase K digestion (but susceptible in the presence of Triton X-100). This demonstrates that the novel protein is contained within the mitochondria. Valinomycin (a K$^+$ ionophore) disrupts membrane potential and, therefore, prevents protein import because import is potential dependent (Winning et al., 1995). Figure 1 demonstrated that very little of the novel protein accumulates in valinomycin-treated
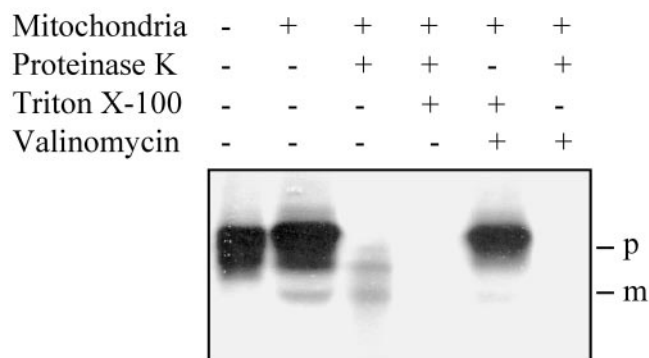
Figure 1. In vitro import of RF2B precursor protein into mitochondria. S^{35}-Met labeled RF2B protein was incubated with purified maize mitochondria, proteinase K, Triton X-100, and/or valinomycin as indicated, subjected to SDS-PAGE, and exposed to x-ray film. p, Precursor RF2B; m, cleaved mitochondrial form of RF2B.

mitochondria. The minor accumulation of the novel protein is presumably the result of incomplete inhibition of import by valinomycin, a finding that has been observed previously (see Rudhe et al., 2002). In combination, these results indicate that a cleaved version of RF2B (i.e. the mature form of RF2B) is imported into mitochondria in vitro (Fig. 1). Hence, these results demonstrate that maize mitochondria contain two ALDHs, i.e. RF2A and RF2B.

Further evidence that the RF2B protein accumulates in mitochondria was obtained via immunoblot analyses. Maize mitochondria were isolated from etiolated seedlings of N cytoplasm Ky21 and similar near-isogenic seedlings that were homozygous for *rf2a-m8122*. Proteins from these mitochondrial preparations were subjected to immunoblot analysis with polyclonal anti-RF2A antibodies, which recognize RF2A and RF2B proteins equally well (Fig. 2A). A cross-reacting protein of the same M_r was detected in both genotypes (Fig. 2B). However, much less of this protein was present in the mitochondrial extract from the mutant seedlings. Because the *rf2a-m8122* mutant contains a *Mu1* transposon insertion in exon 9, plants homozygous for this mutant do not accumulate *rf2a* transcripts (Cui et al., 1996). Hence, the cross-reacting protein detected in mitochondria from the mutant plants cannot be derived from *rf2a*. Similar results were also obtained from *rf2a-m8904* mutants (data not shown), which do not accumulate detectable levels of *rf2a* transcripts (Fig. 2C). Because the RF2A antibodies recognize both RF2A and RF2B recombinant protein expressed in *Escherichia coli* (Fig. 2A), these results provide further support for the mitochondrial localization of RF2B.

Expression of RF2A and RF2B

All studied plant genomes contain two genes that encode mtALDHs. One explanation for this apparent redundancy could be that these two mtALDH genes are differentially regulated. To determine whether this is true for *rf2a* and *rf2b*, the expression patterns of these genes were examined via RNA gel blotting. Both *rf2a* and *rf2b* transcripts accumulate in seedling leaves, seedling roots, silks, husks, ears, and tassels (Fig. 3). However, only *rf2a* transcripts accumulate to detectable levels in adult leaves (Fig. 3).

To examine the accumulation of the RF2A and RF2B proteins, 5-d-old etiolated seedling shoots and root tips were fixed and embedded in LR White resin. Cross sections of shoots and longitudinal sections of root tips were incubated with affinity-purified anti-RF2A IgG and then incubated with gold-labeled sec-
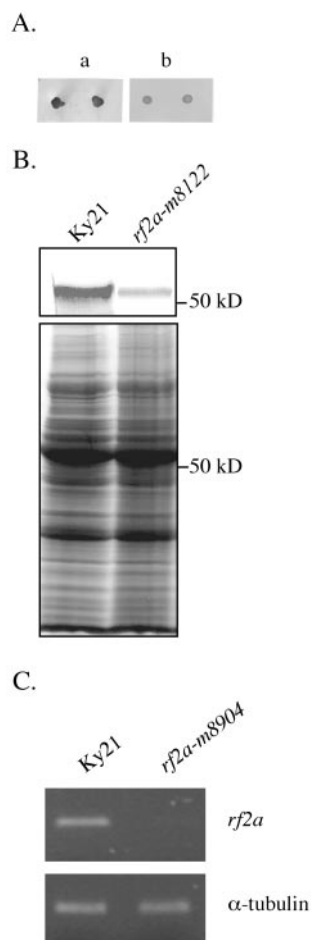
Figure 2. Accumulation of RF2A and RF2B in mitochondria. A, RF2A antibodies recognize both recombinant RF2A and RF2B. Purified recombinant RF2A (left spot) and RF2B (right spot) proteins (0.25 μg) were spotted on nitrocellulose membranes and allowed to react with RF2A antibodies (a) or stained with Coomassie Blue (b). B, Mitochondrial extracts were subjected to SDS-PAGE and then transferred to nitrocellulose membrane. The membrane was sequentially incubated with rabbit anti-RF2A IgG, alkaline phosphate-conjugated goat anti-rabbit IgG monoclonal antibody, and nitroblue tetrazolium/5-bromo-4-chloro-3-indolyl phosphate solutions. Each lane contains 150 mg of total mitochondrial protein. A duplicate Coomassie Blue-stained polyacrylamide gel is shown below as a loading control. C, Accumulation of *rf2a* transcripts in *rf2a-m8904* mutant plants as analyzed by RT-PCR. α-Tubulin serves as a control.

A.

B.
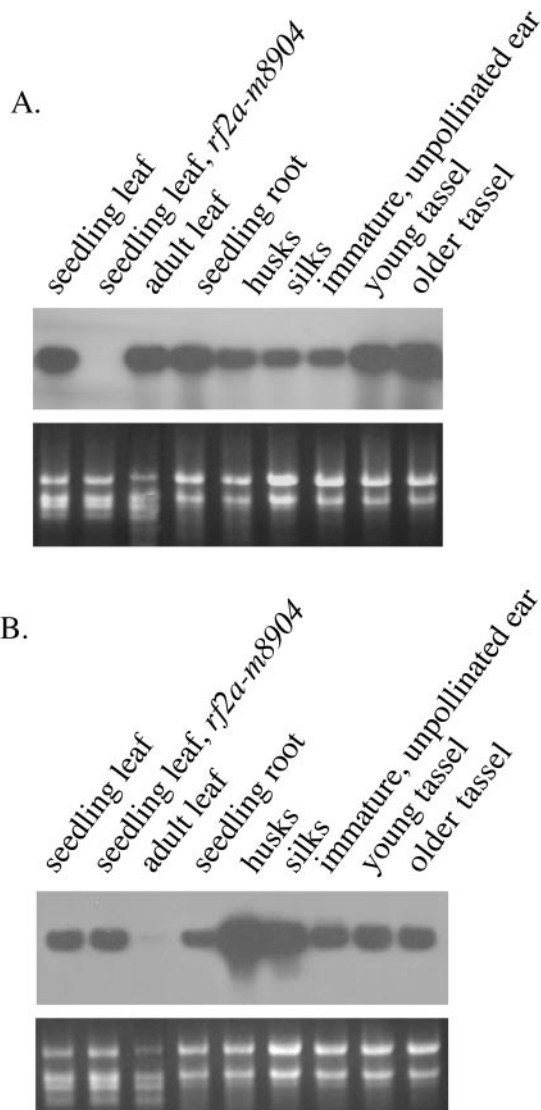
Figure 3. RNA gel-blot analyses of *rf2a* and *rf2b* transcripts. A, *rf2a*; B, *rf2b*. Unless otherwise indicated, all RNA was extracted from the inbred line Ky21. Each lane contained 15 μg of RNA. RNA gel blots were hybridized with ^{32}P-labeled *rf2a-* and *rf2b*-specific probes, respectively. Ethidium bromide-stained rRNAs are shown below as loading controls.

ondary antibody. The gold signal was enhanced by silver salt.

These immunolocalization analyses were conducted on N cytoplasm Ky21 and a near-isogenic version of Ky21 that is homozygous for *rf2a-m8904*. Because the RF2A antibodies can recognize both RF2A and RF2B (Fig. 2), the signal detected in Ky21 is the sum of RF2A and RF2B accumulation. Because the *rf2a-m8904* mutant contains a *Ds1* transposon insertion in exon 1 downstream of the translation start codon, plants homozygous for this mutant do not accumulate detectable levels of *rf2a* transcript (Cui et al., 1996) or RF2A (Liu et al., 2001). Hence, the

signal detected in plants homozygous for *rf2a-m8904* reflects the accumulation of only RF2B.

The signal detected in Ky21 seedling shoots is present mainly in photosynthetic cells, including the bundle sheath cells and mesophyll cells (Fig. 4A). Little signal was detected in epidermal cells and very little, if any, signal was detected in the coleoptile (data not shown), or vascular bundle cells (Fig. 4A). Less signal, but with a similar distribution, was detected in the *rf2a-m8904* shoots (Fig. 4B).

In the root tip, the signal was highest in the root cap, including all the root cap cells; very little signal was found in the meristem or elongation zone (Fig. 4C). In the *rf2a-m8904* root tips, the signal derived from RF2B was found only in young root cap cells, i.e. those closest to the calyptrogen cells, which generate all root cap cells (Fig. 4D). As in Ky21, no signal was detected in cells within the meristem or the elongation zone.

Expression and Purification of Recombinant RF2A and RF2B

The *rf2a* and *rf2b* cDNAs were cloned into the expression vector pET17b and expressed in *E. coli* (Liu et al., 2001; Skibbe et al., 2002). *E. coli*-expressed RF2A was purified using cellulose DE52 anion-exchange chromatography, Sephadex G-50 gel filtration, and hydroxyapatite and NAD-agarose affinity columns (see "Materials and Methods" for details). The RF2B protein was purified using cellulose DE52 anion-exchange chromatography, Sephadex G-50, and hydroxyapatite and Blue-Cibracon GF-3A columns ("Materials and Methods"). After the final step in each purification procedure, only a single major band was visible on a Coomassie Blue-stained SDS gel (Fig. 5). The purification schemes of both enzymes are shown in Table I. RF2A was purified about 40-fold and RF2B about 60-fold. Purified recombinant RF2A and RF2B proteins can be stored in −20°C in 25% (v/v) glycerol for at least 15 months without apparent loss of activity.

After the elution of RF2A and RF2B from the cellulose DE52 column, the pooled ALDH-containing fractions were desalted using Sephadex G-50 before loading the hydroxyapatite column. This desalting step often caused a loss of ALDH activity, perhaps as a consequence of the low ionic strength (20 mM) of the buffer. Regardless of the cause, the addition of 10% (v/v) glycerol significantly stabilized the ALDH activity, although the specific activity still decreased somewhat during this step (Table I).

Biochemical Characterization of RF2A and RF2B

As determined via Sephacryl S-300 chromatography ("Materials and Methods"), the molecular masses of RF2A and RF2B are 214 and 200 kD, respectively. As discussed above, the mitochondrial
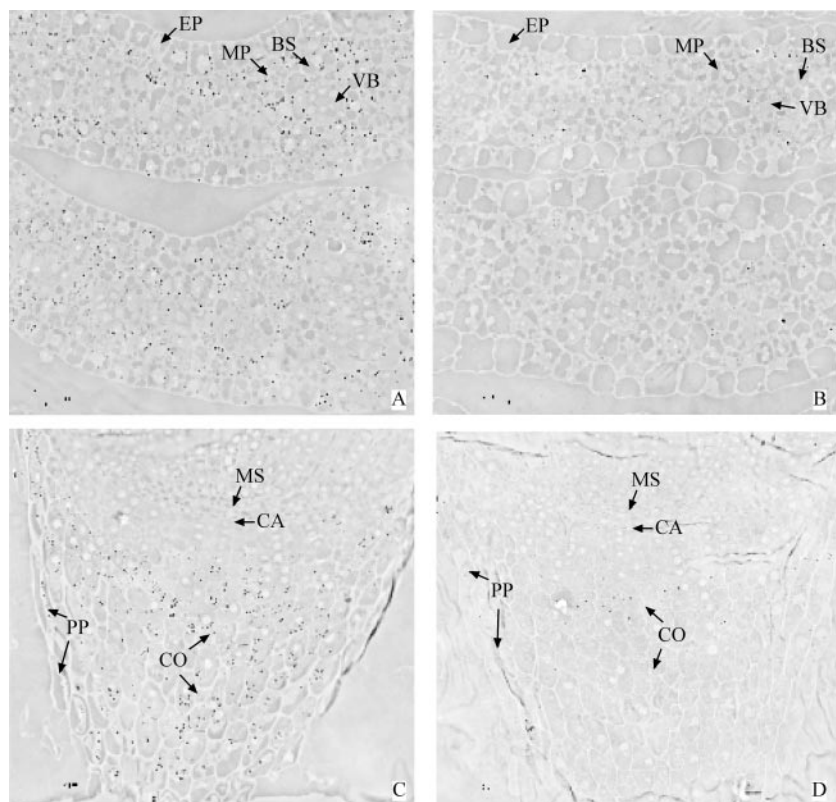
Figure 4. Immunolocalization of RF2A and RF2B proteins. A, Cross section of shoot from a 5-d-old Ky21 seedling that is homozygous for the RF2A-Ky21 and RF2B-Ky21 alleles. B, Cross section of shoot from a 5-d-old seedling that is homozygous for *rf2a-m8904* and RF2B-Ky21 allele, and that is nearly isogenic with Ky21. C, Longitudinal section of the root tip from a 5-d-old Ky21 seedling. D, Longitudinal section of root tip from a 5-d-old seedling with the same genotype as B. All sections were incubated with affinity-purified rabbit anti-RF2A antibodies, followed by gold-labeled goat anti-rabbit IgG antibodies and silver enhancement and viewed under a light microscope using phase contrast. EP, Epidermis; MP, mesophyll cells; BS, bundle sheath cells; VS, vascular tissue; PP, peripheral cells; MS, root meristem; CA, calyptrogen cells; CO, columella cells.

targeting sequence of RF2A is cleaved between residues Ser-50 and Thr-51 and the targeting sequence of RF2B is predicted to be cleaved between Ser-47 and Thr-48. Using these cleavage sites and the pI/Mw program (http://ca.expasy.org/tools/pi_tool.html), the molecular masses of single subunits of RF2A and RF2B are estimated to be 54.2 and 54.0 kD, respectively. These results demonstrate that both RF2A and RF2B exist as homotetramers, as is true for the mtALDHs of mammals (Hart and Dickinson, 1977) and yeast (Tamaki et al., 1978). It is not possible to exclude the possibility that RF2A and RF2B form heterotetramers in vivo.

Under normal physiological conditions, the pH of the mitochondrial matrix is usually greater than 8.0, but it undergoes changes in response to various environmental conditions (Salvador et al., 2001). To determine whether RF2A and RF2B exhibit ALDH activity at these physiological conditions, the effects of changes in pH on the ALDH activities of both proteins were investigated. A series of 0.1 M phosphate buffers and pyrophosphate buffers were used to provide the desired pH conditions. The pH optima for RF2A and RF2B are 9.0 and 7.5, respectively (Fig. 6A). At pH 8.0, the activity of RF2B was near its maximal value; in contrast, RF2A exhibited only about one-half of its maximal activity at this pH.

The activity of many enzymes increases in proportion to substrate concentration until the enzyme is saturated with substrate, at which point activity plateaus. ALDHs, on the other hand, often exhibit a phenomenon termed substrate inhibition (Sidhu and Blair, 1975). When substrate concentration increases beyond a certain level, ALDH activity typically decreases. To investigate whether RF2A and RF2B are subject to substrate inhibition, RF2A and RF2B activities were tested with a series of acetaldehyde concentrations. Although both proteins exhibit substrate inhibition, RF2A is inhibited at lower aldehyde concentrations and exhibits more inhibition than does RF2B (Fig. 6B). RF2A and RF2B began to exhibit substrate inhibition when the concentrations of acetaldehyde reached 180 μM and 18 mM, respectively.

Typical mtALDHs exhibit esterase activity in vitro (Weiner et al., 1976). Esterase (E.C. 3.1.1.1) catalyzes the conversion of carboxylic esters into the corresponding alcohols and carboxylic anions. To investigate whether this is also true for RF2A and RF2B, an esterase assay was conducted on purified recombinant RF2A and RF2B. Both RF2A and RF2B exhibited esterase activity against 4-nitrophenyl acetate, with similar catalytic rates (Fig. 6C).

Mammalian mtALDHs are inhibited by disulfiram (Lam et al., 1997), the active component in some drugs used to treat alcoholism. To determine whether RF2A and RF2B are similarly inhibited by disulfiram, each enzyme was incubated with 0.5 mM disulfiram at room temperature for 15 min before conducting ALDH assays. Acetaldehyde (17.9 μM) was used as substrate. As shown in Figure 6D, disulfiram inhibited RF2B activity nearly 90%. In contrast, disulfiram inhibited RF2A activity by only
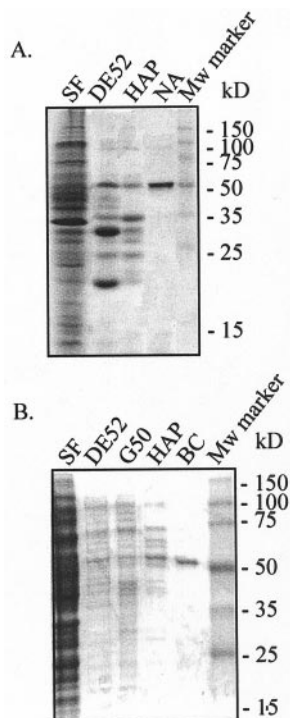
Figure 5. Purification of recombinant RF2A and RF2B from *E. coli*. A, RF2A; B, RF2B. For both A and B, pooled ALDH-containing fractions from each step were subjected to SDS-PAGE and stained with Coomassie Blue R-250. SF, Soluble fractions of extracts from *E. coli* that carry pMAP11 or pRB17; DE52, ALDH-containing fractions from cellulose DE52 columns (Whatman, Clifton, NJ); HAP, ALDH-containing fractions from hydroxyappitite columns; NA, ALDH-containing fractions from NAD-agarose columns; G50, ALDH fractions from Sephadex G50 columns; BC, ALDH-containing fractions from Blue-Cibracon GF-3A affinity columns.

about 20%. Hence, RF2B is substantially more susceptible to disulfiram inhibition than is RF2A.

While conducting kinetic analyses, it was found that RF2A exhibits positive cooperativity toward some aldehydes (Fig. 6E); RF2B does not. Positive cooperativity occurs when a protein has multiple substrate-binding sites and the binding of one molecule of substrate causes conformation changes in the enzyme that favor the binding of additional substrate molecules. The degree of cooperativity is expressed as the Hill coefficient. RF2A has Hill coefficients around 3 for saturated aliphatic and some aromatic aldehydes (Table II). Although mtALDHs and cALDHs from mammals and yeast are also homotetramers, we are not aware of any previous reports that these enzymes exhibit cooperativity. Hence, to our knowledge, RF2A appears to be the first natural ALDH reported to exhibit positive cooperativity.

## Kinetic Analyses of RF2A and RF2B

An analysis of RF2A's substrate specificity has the potential to help to identify the specific biochemical pathway in which it functions during fertility restoration and normal anther development. Comparisons of the substrate specificities of RF2A and RF2B might help define why all studied plant genomes contain two mtALDH genes. Toward these ends, purified recombinant RF2A and RF2B proteins were subjected to kinetic analyses. The results are shown in Table II.

The ratio of K_{cat} to K_m can be used to estimate an enzyme's overall specificity and affinity toward a particular potential substrate. The majority of the tested aldehydes can serve as substrates for RF2A. Most saturated aliphatic aldehydes (i.e. acetaldehyde, propionaldehyde, butyraldehyde, valeraldhyde, hexanal, heptaldehyde, octanal, and nonanal), aromatic aldehydes (i.e. benzaldehyde and some of its derivatives, such as 4-nitrobenzaldehyde, anisaldehyde, cinnamaldehyde, and *o*-nitrocinnamaldehyde) and other aldehydes (acrolein, chloroacetaldehyde, glycolaldehyde, and indole-3-acetaldehyde) have K_ms in the low micromolar range and K_{cat}s in the range of 10 to 100 per second. In contrast, relatively few aldehydes serve as substrates for RF2B; substrates are limited to the short-chain aliphatic aldehydes acetaldehyde, propionaldehyde, and butyraldehyde. Based on the ratio of K_{cat} to K_m, the best substrate for RF2A is acetaldehyde; the next best substrates are propionaldehyde, *o*-nitrocinnamaldehyde, butyraldehyde, 4-nitrobenzaldehyde, and *m*-anisaldehyde.

Table I. *Purification of recombinant RF2A and RF2B*

One unit of enzyme activity (U) is expressed as 1 μmol of NADH min^{-1}. Specific activity is expressed as unit activity mg protein^{-1}. Purification fold is expressed as increased specific activity normalized by specific activity from the soluble extract. The data presented represent one typical experiment.

	Soluble Fraction	DE52	G50	HAP	NAD-Agarose	BC
RF2A						
Total protein (mg)	202	90.0	66.2	5.70	0.700	–
Total activity (U × 10³)	29.0	25.7	12.2	6.70	3.66	–
Specific activity (U mg⁻¹)	144	285	184	1,180	5,230	–
Purification fold	–	2.2	1.4	8.2	36	–
RF2B						
Total protein (mg)	334	20.8	15.0	5.2	–	0.41
Total activity (U × 10³)	102	53.6	38.1	26.7	–	7.46
Specific activity (U mg⁻¹)	306	2,580	2,540	5,140	–	18,200
Purification fold	–	8.4	8.3	17	–	60

A.

B.

C.

D.

E.
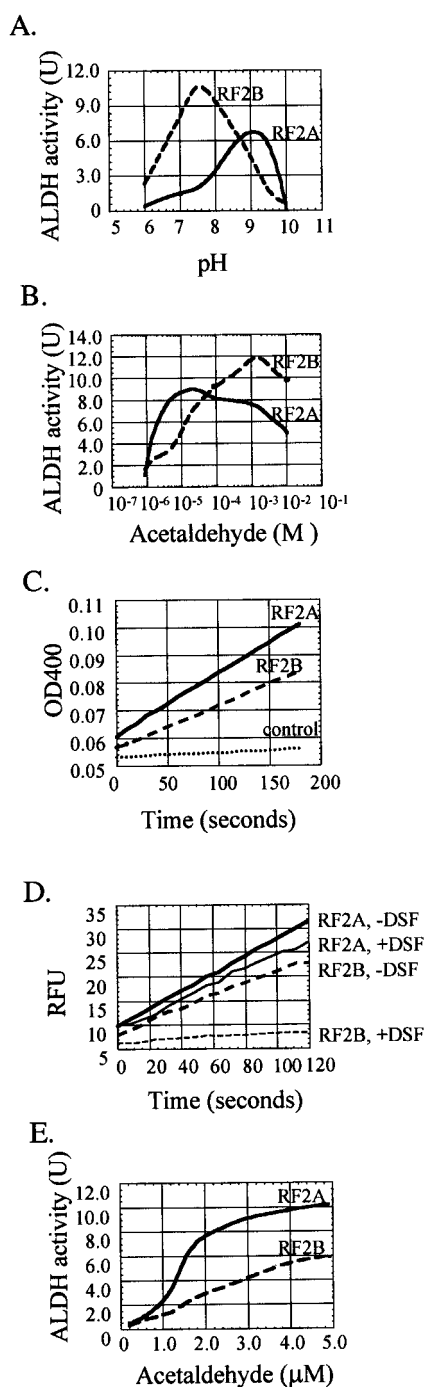
Figure 6. Biochemical characterizations of RF2A and RF2B. A, pH optima. pH 6.0 to 8.0 buffer was 0.1 M sodium phosphate; pH 8.5 to 9.5 buffer was 0.1 M tetrasodium pyrophosphate; pH 10.0 buffer was sodium bicarbonate-carbonate. B, Substrate inhibition. For both RF2A and RF2B, assays were conducted in 0.1 M tetrasodium pyrophosphate buffer, pH 8.5. C, Esterase activity. Assays were conducted in 50 mM sodium phosphate buffer (pH 7.4); 125 μM phenylacetate was used as substrate. The control is the assay mixture without enzyme. D, Disulfiram inhibition. RF2A and RF2B were incubated with (+DSF) or without (−DSF) 0.5 mM disulfiram for 15 min before ALDH assay. E, Positive cooperativity of RF2A. All assays were conducted at room temperature and used 18 μM acetaldehyde, 2 μg of RF2A, or 1 μg of RF2B unless otherwise indicated.

Excluding trans-2-nonenal, indole-3-carboxyaldehyde, and 2-naphthaldehyde, 9-cis-retinal and all-trans-retinal, which RF2A cannot oxidize, its five worst substrates are trans-2-hexenal, formaldehyde, decylaldehyde, pyruvic aldehyde, and citral.

Increased cellular levels of reactive oxygen species (ROS) can lead to lipid peroxidation (for review, see Comporti, 1989) and the accumulation of short- to medium-chain saturated aldehydes and α,β-unsaturated aldehydes. The abilities of RF2A and RF2B to oxidize three α,β-unsaturated aldehydes (trans-2-hexenal, trans-2-nonenal, and 4-HNE) that are associated with lipid peroxidation were tested. RF2A can oxidize trans-2-hexenal, with a K_m of 56 μM, but a K_{cat} of only 5.2 s^{-1} (5% of the K_{cat} of its best substrate, acetaldehyde); for 4-HNE, the K_m is 1.1 μM and the K_{cat} is 4.3 s^{-1} (4% of the K_{cat} of acetaldehyde). Because of its low K_m, RF2A's K_{cat} to K_m ratio for 4-HNE is only 1.2. RF2A does not oxidize trans-2-nonenal; the addition of a hydroxyl group at fourth position (4-HNE) apparently changes the affinity of the aldehyde to RF2A dramatically. RF2B cannot oxidize any of the tested α,β-unsaturated aldehydes that are associated with lipid peroxidation.

Overall, RF2A has a broad substrate spectrum, whereas RF2B functions on a rather limited group of aldehydes, i.e. aliphatic aldehydes with chain lengths shorter than five carbons. No significant RF2B activity was detected toward aliphatic aldehydes with chain lengths greater than six carbons, any of the aromatic aldehydes, or other aldehydes listed in Table II.

A number of ALDHs can use both NAD$^+$ and NADP$^+$ as coenzymes. RF2A and RF2B both use only NAD$^+$. The K_ms for NAD$^+$ with RF2A and RF2B are 0.19 and 0.04 mM, respectively. No activity was detected for either enzyme when NADP$^+$ was used as coenzyme (data not shown).

Levels of ROS and Lipid Peroxidation in N and T Cytoplasm Anthers

cms in sunflower (*Helianthus annuus*) is associated with programmed cell death (Balk and Leaver, 2001). Programmed cell death is associated with increased levels of ROS and subsequent lipid peroxidation (for review, see Gamaley and Klyubin, 1999; Jabs, 1999). To determine whether sterility in T-cytoplasm maize occurs via a similar process, the levels of ROS and lipid peroxidation were measured in maize anthers.

The levels of ROS were compared between anthers from N and T cytoplasm plants that were homozygous for *rf2a-m8904*. ROS levels were detected by staining anthers with an ROS-specific fluorescent dye 2,7-dichlorofluorescin 3,6-diacetate (DCFDA). DCFDA per se does not fluoresce, but this probe can be diffused into cells and endogenous esterases convert it into 2,7-dichlorofluorescin, which can be oxidized by cellular hydrogen peroxide and hydroxyl
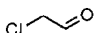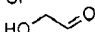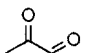
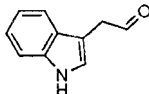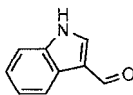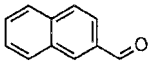**Table II.** *Kinetic analyses of RF2A and RF2B*

ALDH activities of purified recombinant RF2A and RF2B proteins were assayed with a series of substrate concentrations for each aldehyde to determine the K_m and K_{cat}. Data represent averages from at least three experiments.

Substrate	Substrate Structure	K_m[a]		K_{cat}		Hill Coefficient	K_{cat}/K_m	
		RF2A	RF2B	RF2A	RF2B	RF2A	RF2A	RF2B
		µM		s^{-1}				
Saturated aliphatic aldehydes								
Formaldehyde		110 ± 20	540 ± 90	4.3 ± 0.3	15 ± 1	NC[b]	0.39	0.03
Acetaldehyde		2.4 ± 0.7	6.6 ± 0.8	100 ± 3	100 ± 27	2.8 ± 0.6	43	23
Propionaldehyde		3.5 ± 0.5	5.4 ± 0.7	72 ± 13	130 ± 15	3.1 ± 0.7	21	25
Butyraldehyde		3.1 ± 0.6	2.6 ± 0.5	46 ± 3	120 ± 21	3.1 ± 0.3	18	43
Valeraldehyde		1.5 ± 0.3	Trace[c]	9.5 ± 2	–[d]	3.2 ± 0.7	6.2	–
Hexanal		2.0 ± 0.2	–	11 ± 2	–	3.7 ± 0.2	5.6	–
Heptaldehyde		4.6 ± 1.0	–	30 ± 2	–	2.1 ± 0.9	6.5	–
Octanal		7.3 ± 1.0	–	23 ± 3	–	3.9 ± 0.1	3.0	–
Nonanal		9.5 ± 2.0	–	19 ± 3	–	3.0 ± 1.5	2.0	–
Decylaldehyde		15 ± 0.4	–	14 ± 1	–	3.9 ± 0.2	0.92	–
Aromatic aldehydes								
Benzaldehyde		3.4 ± 0.9	–	30 ± 3	–	1.8 ± 0.8	8.8	–
4-Nitrobenzaldehyde		7.4 ± 2.0	–	10 ± 2	–	3.1 ± 0.3	14	–
p-Anisaldehyde		0.9 ± 0.1	–	1.8 ± 0.1	–	NC	6.5	–
m-Anisaldehyde		2.1 ± 0.03	–	5.9 ± 1	–	NC	14	–
Trans-cinnamaldehyde		3.5 ± 0.3	–	31 ± 3	–	NC	8.8	–
o-Nitrocinnamaldehyde		3.0 ± 1.0	–	59 ± 6	–	NC	19	–
Unsaturated aliphatic Aldehydes								
Acrolein (propenal)		13 ± 1	–	36 ± 3	–	NC	2.7	–
trans-2-hexenal		55 ± 7	–	5.2 ± 1	–	NC	0.10	–
trans-2-nonenal		–	–	–	–	NC	–	–
4-Hydroxy-2-nonenal (4-HNE)		1.1 ± 0.3	–	4.3 ± 1	–	NC	3.9	–
						–		–
Citral		3.0 ± 0.9	–	4.6 ± 0.6	–	NC	1.5	
Retinal aldehydes								
9-*cis*-retinal		–	–	–	–	–	–	–
All-*trans*-retinal		–	–	–	–	–	–	–

(*Table continues on facing page.*)

Table II. (*Continued from preceding page.*)

Substrate	Substrate Structure	$K_m{}^a$		K_{cat}		Hill Coefficient	K_{cat}/K_m	
		RF2A	RF2B	RF2A	RF2B	RF2A	RF2A	RF2B
		μM		s^{-1}				
Other aldehydes								
Chloroacetaldehyde		11 ± 1	–	72 ± 3	–	NC	6.5	–
Glycolaldehyde		9.6 ± 2	500 ± 130	100 ± 12	153 ± 26	NC	11	0.29
Pyruvic aldehyde		4.9 ± 1	–	6.2 ± 0.3	–	NC	1.2	–
Indole-3-acetaldehyde		5.0 ± 1	–	8.2 ± 3	–	NC	1.7	–
Indole-3-carboxyaldehyde		–	–	–	–	–	–	–
2-Naphthaldehyde		–	–	–	–	–	–	–

[a] K_m should be "apparent K_m" for those substrates that show positive cooperativity. [b] NC, No cooperativity was observed with aldehyde substrate. [c] Trace, Only trace activity detected with 10 μg of purified enzyme. [d] ALDH activity not detected with various aldehyde concentrations and in the presence of at least 10 μg of purified enzyme.

free radicals, thereby generating 2,7-fluorescein. 2,7-Fluorescein can be detected by excitation at 495 nm and emission at 525 nm (Royall and Ischiropoulos, 1993). As shown in Figure 7, at the same stage of development, there is no difference in the amount of fluorescence observed from anthers of the two genotypes. This indicates that ROS levels are similar in N and T cytoplasm anthers. Interestingly, the younger anthers of both genotypes fluoresce more strongly than the older anthers, suggesting that anthers accumulate higher levels of ROS at the meiocyte than the early microspore stage of development.

The levels of lipid peroxidation were measured in anthers from four nearly congenic maize lines: N cytoplasm Ky21 plants, and closely related N cytoplasm plants homozygous for *rf2a-m8904*, T cytoplasm Ky21 plants, and closely related T cytoplasm plants homozygous for *rf2a-m8904*. All but the last of these lines are male fertile. The lipid peroxidation assay is based on the detection of malondialdehyde (MDA), a major product of lipid peroxidation (Esterbauer et al., 1991). In the presence of hydrochloric acid, MDA can react with *N*-methyl-2-phenylindole to form a chromogenic compound, which exhibits maximum A_{586} (Botsoglou et al., 1994). As shown in Table III, there are no significant differences in levels of MDA among the four genotypes.

ALDH Activity of Native RF2B

Access to an *rf2a* null mutant *rf2a-m8122* makes it possible to assay the ALDH activity of native RF2B. As mentioned above, homozygous *rf2a-m8122* mutant plants do not accumulate *rf2a* transcripts (Cui et

al., 1996). Therefore, if maize, like all other eukaryotes analyzed to date, contains only two mtALDHs, any ALDH activity detected in mitochondria from plants homozygous for *rf2a-m8122* must be derived from RF2B. The assumption that the maize genome contains only two mtALDH genes (*rf2a* and *rf2b*) is consistent with our analyses of extensive public and private sector maize expressed sequence tag databases (Skibbe et al., 2002; data not shown). Hence, the difference in the ALDH activities of mitochondrial extracts from Ky21 plants and near-isogenic plants that are homozygous for *rf2a-m8122* provides an estimate of the ALDH activity of RF2B. Estimating RF2B activity via this approach requires the assumption that RF2B activity is not affected by RF2A accumulation.

Mitochondria were purified from etiolated seedlings and ALDH activities were assayed using glycolaldehyde and acetaldehyde as substrates. As shown in Table II, the K_m of glycolaldehyde for RF2B (approximately 500 μM) is substantially higher than that for RF2A (approximately 10 μM). Therefore, and again assuming that maize has only two mtALDHs, any glycolaldehyde dehydrogenase activity observed in mitochondrial extracts at low concentrations of glycolaldehyde must be derived from RF2A. If RF2B accumulates in mitochondria, the ratio of mtALDH activity in mitochondrial extracts from *rf2a* mutants and Ky21 should be higher at high glycolaldehyde concentrations than at low concentrations. This is because RF2B exhibits ALDH activity only at high concentrations of glycolaldehyde.

The results of these mtALDH assays are shown in Table IV. When ALDH assays were conducted with
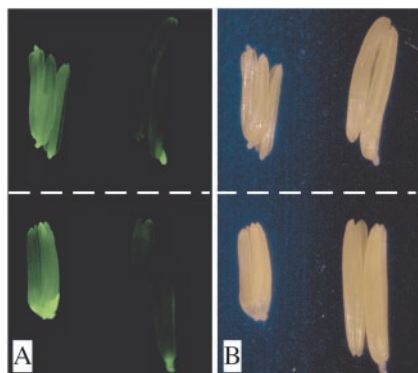
Figure 7. Determination of ROS levels in maize anthers. A, Anthers visualized under fluorescent light; B, the same anthers visualized under white light. Anthers were dissected from plants homozygous for *rf2a-m8904* but otherwise nearly congenic with the inbred line Ky21. Anthers above the dashed line were harvested from a T cytoplasm plant; anthers below the dashed line were from an N cytoplasm plant. The smaller and larger anthers were at the meiocyte and early microspore stages, respectively. Anthers were stained with DCFDA. Fluorescence reflects ROS levels. The fluorescence in the filaments at the base of the anthers reveals the increased levels of ROS that accumulated following the wounding that occurred when the anthers were excised from their florets.

20 μM glycolaldehyde, the mitochondrial extracts from *rf2a* mutant seedlings exhibited only about 27% of the ALDH activity observed in mitochondrial extracts from Ky21 plants. However, when the concentration of glycolaldehyde was increased to 4.0 mM, the *rf2a* mutant exhibited about 50% of the mtALDH activity observed in Ky21 extracts. Because RF2A activity is partially inhibited at 4 mM glycolaldehyde (Fig. 6B; data not shown), this experiment probably underestimates the ALDH activity of RF2B. As a control, this dramatic increase in mtALDH activity was not observed when increasing concentrations of acetaldehyde were used as substrate; this is consistent with the finding that the K_ms of acetaldehyde for RF2A and RF2B are similar (Table II). Hence, this experiment demonstrates that mitochondria contain RF2B-dependent glycolaldehyde dehydrogenase activity and that the kinetic assays using recombinant RF2A and RF2B reflect the kinetic characteristics of native RF2A and RF2B enzymes.

Structures of RF2A and RF2B

The overall levels of amino acid similarity and identity between RF2A and RF2B are 83% and 79%, respec-

Table III. *Lipid peroxidation assay of maize spikelets*

MDA concentrations are expressed as μM mg protein^{-1}. Data represent the averages of two parallel experiments.

Genotype	MDA Concentration
(N)Ky21	16.4 ± 0.9
(N)*rf2a-m8904*	15.8 ± 1.2
(T)Ky21	17.9 ± 2.1
(T)*rf2a-m8904*	17.0 ± 2.6

Table IV. *ALDH assays of maize mitochondrial preparations*

Mitochondria were purified from etiolated maize seedlings of the inbred line Ky21 or homozygous for *rf2a-m8122* and ALDH assays were conducted as described in "Materials and Methods." The data represent the average from two parallel experiments; in each experiment, ALDH activity was measured three times for each substrate concentration. ALDH activity is expressed as μmol NADH min mg protein^{-1}.

Substrate	Substrate Concentration	Ky21	*rf2a-m8122*
Glycolaldehyde	20 μM	12 ± 0.1	3.2 ± 0.4
	4.0 mM	16 ± 2	7.8 ± 0.5
Acetaldehyde	18 μM	18 ± 0.1	6.8 ± 0.8
	1.8 mM	17 ± 4	8.1 ± 0.1

tively. To begin to determine which amino acids might be responsible for the dramatic differences in the substrate specificities and other kinetic characteristics of these two enzymes, the leader sequence of RF2A and putative leader sequence of RF2B were trimmed, and the mature protein sequences were submitted to Swiss-model (http://www.expasy.ch/swissmod/SWISS-MODEL.html; Peitsch et al., 2000) for three-dimensional structural predictions. Because RF2A and RF2B have similar predicted three-dimensional structures (Fig. 8), it appears that relatively subtle differences are responsible for the differences in substrate specificities and other kinetic characteristics of these two mtALDHs.

As a first step toward determining which amino acid residues might be responsible for these differences in substrate specificities and other kinetic characteristics, the sequences of RF2A; RF2B; the two mtALDHs from rice, OsALDH2A (GenBank accession no. AB030939) and OsALDH2B (GenBank accession no. AB044537); and the two mtALDHs from sorghum, SbALDH2a (GenBank accession no. AB084897) and SbALDH2b (GenBank accession no. AB084898) were aligned (Fig. 9). According to phylogenetic analyses (Fig. 10), OsALDH2B and SbALDH2B are most closely related to maize RF2A (GG1) and OsALDH2A and SbALDH2A are most closely related to maize RF2B (GG2). The clustering of GG1 and GG2 mtALDHs was supported in 85 of 100 independent bootstrap experiments. The algorithm pSORT (http://psort.nibb.ac.jp; Nakai and Kanehisa, 1992) detects a putative mitochondrial targeting sequence motif in each of the grass mtALDHs. For the GG1 mtALDHs (OsALDH2B, SbALDH2B, and RF2A), this motif is QRFST; for the GG2 mtALDHs (OsALDH2A, SbALDH2A, and RF2B), the motif is HRFS(T/A). The predicted cleavage site for both the GG1 and GG2 mtALDHs is after amino acid position 64 of the consensus sequence shown in Figure 9 (index no. 64).

Between position 64 and the carboxyl terminus, there are 15 amino acid residues that are conserved within GG1 and within GG2, but that differ between
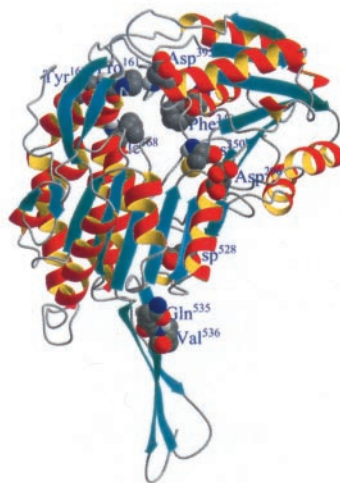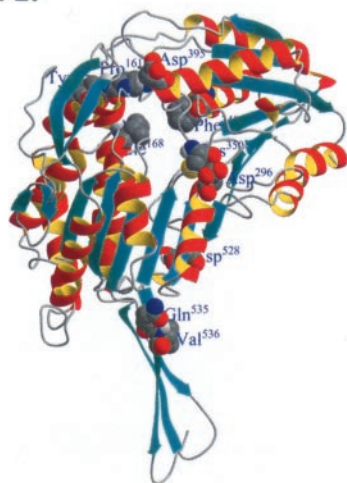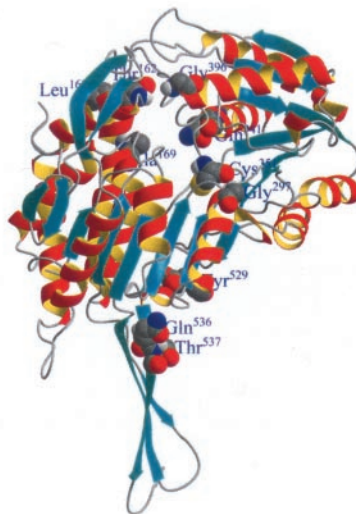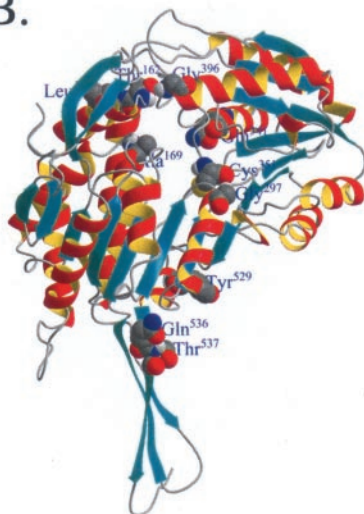
Figure 8. Predicted three-dimensional structures of RF2A and RF2B. Structures were predicted by SWISS-MODEL (Guex and Peitsch, 1997) and cross-eyed stereo images were prepared with MOLMOL software (Koradi et al., 1996). A, RF2A; B, RF2B. Pro-161/Thr-162, Tyr-162/Leu-163, Asp-395/Gly-396, Asp-296/Gly-297, and Asp-529/Tyr-530 substitutions are conserved between Grass Group 1 (GG1) RF2A/OsALDH2B/SbALDH2B) and Grass Group 2 (GG2) RF2B/OsADLH2A/SbALDH2A) and are located around the substrate pockets. Residues Ile-168/Ala-169 and Phe-340/Gln-341 are not conserved between the two groups but are also located on the surface of the substrate pocket and may play roles in defining substrate specificity. The catalytic Cys (Cys-350/Cys-351) is shown in both images. Gln-535/Gln-536 is equivalent to the human (*Homo sapiens*) "oriental mutation" E487K, which is believed to be involved in subunit interaction. Val-536/Thr-537 is the amino acid next to it and this substitution is also conserved between the two groups of mtALDHs.

GG1 and GG2. Five of these residues are located either within the catalytic domain or on the surface of the substrate-binding pocket. Pro-161/Thr-162 (RF2A/RF2B), Tyr-162/Leu-163, and Asp-395/Gly-396 are located on the top of the substrate-binding pocket; Asp-296/Gly-297 is located in one of the NAD-binding domains, which is also located at the entrance of the substrate pocket; and Asp-529/Tyr-530 is located at the bottom of the substrate pocket, which is only three amino acids away from a Glu (index no. 535, Fig. 9, equivalent to Glu-476 in bovine ALDH2; Steinmetz et al., 1997) that may be involved in binding of a water molecule and facilitating acyl-enzyme hydrolysis (Steinmetz et al., 1997).

Because they are located within the substrate pocket, two additional amino acid substitutions between RF2A and RF2B (Ile-168/Ala-169 and Phe-340/Gln-341) are potentially functionally important, even though they are not conserved within GG1 and

GG2 ALDHs. Because the two residues that are present in RF2A at these positions (Ile-168 and Phe-340) are bulky and hydrophobic as compared with the two in RF2B (Ala-169 and Gln-341), they have the potential to affect substrate specificity.

DISCUSSION

The Physiological Functions of RF2A

Since the discovery that the nuclear restorer gene *rf2a* encodes a mtALDH (Cui et al., 1996; Liu et al., 2001), efforts have been focused on identifying its physiological role in restoration of fertility to cmsT maize and in normal anther development. We have hypothesized previously that RF2A's specific role in fertility restoration may involve α-oxidation, protecting plants from the damaging effects of lipid peroxidation, indole-3-acetic acid (IAA) biosynthesis, or
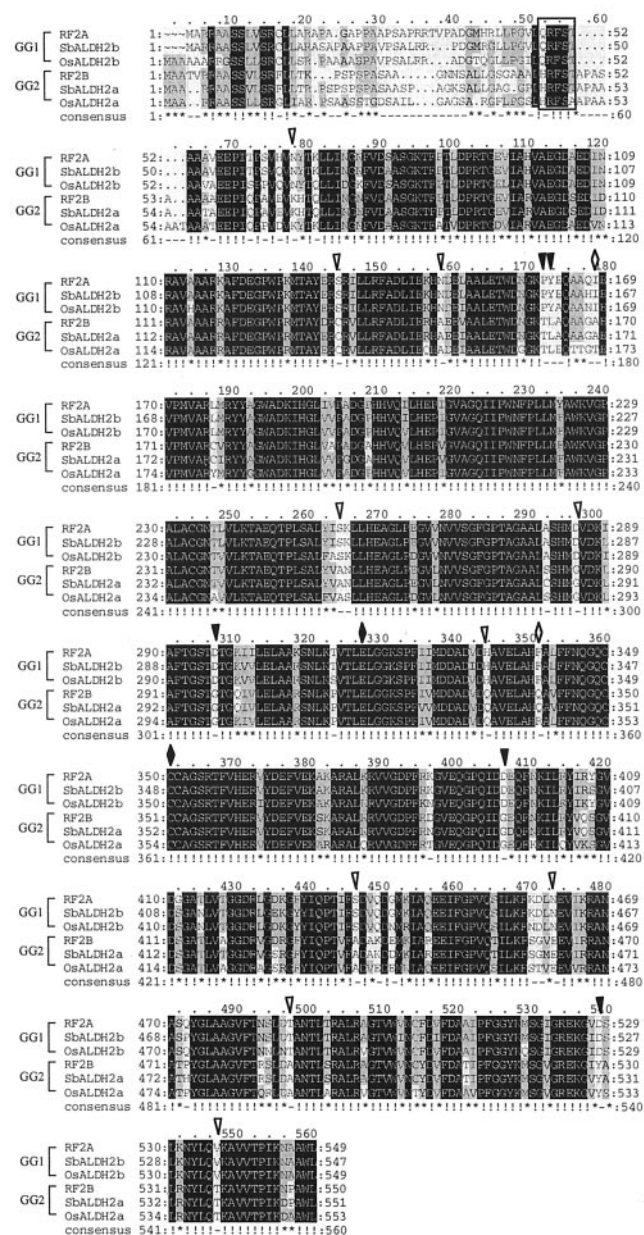
Figure 9. Amino acid alignment of grass mtALDHs. The mitochondrial motifs predicted by pSORT (http://psort.nibb.ac.jp/) are boxed. Black triangles indicate the five conserved amino acid substitutions between GG1 and GG2 mtALDHs that are located around the substrate pockets as shown in Figure 8; white triangles indicate other conserved amino acid substitutions between GG1 and GG2. The catalytic Cys and Glu are indicated by black diamonds. Ile-168/Ala-169 and Phe-340/Gln-341 are indicated by white diamonds. Sb, Sorghum; Os, rice.

ethanolic metabolism (Cui et al., 1996; Liu et al., 2001). The kinetic analyses reported here provide a means to begin to evaluate these hypotheses.

α-Oxidation

α-Oxidation of fatty acids generates a fatty aldehyde intermediate that must be oxidized by an ALDH. Although RF2A can oxidize aldehydes with chain lengths of up to 10 carbons, its K_{cat} to K_m ratio decreases as aldehyde chain lengths increase (Table II). The K_{cat} to K_m ratio for decyl aldehyde is only 0.92, making it one of the worst substrates for RF2A. In addition, α-oxidation occurs in peroxisome (Jansen et al., 2001), whereas RF2A is located in mitochondria. Therefore, it is unlikely that RF2A plays a significant role in α-oxidation.

Lipid Peroxidation

Male sterility is associated with programmed cell death in sunflower (Balk and Leaver, 2001), a process that is associated with oxidative stress and subsequent lipid peroxidation (for review, see Gamaley and Klyubin, 1999; Jabs, 1999). It has been suggested by us (Liu et al., 2001) and others (Møller, 2001) that RF2A might be involved in the detoxification of aldehydes generated by lipid peroxidation after the formation of ROS. This study revealed that RF2A is not an efficient enzyme for detoxifying the α,β-unsaturated aldehydes generated by lipid peroxidation. Although RF2A is able oxidize three- to nine-carbon aliphatic aldehydes that can be produced during lipid peroxidation, its efficiency decreases as carbon chain lengths increase (Table II). Given these kinetic data and our findings that the levels of ROS and lipid peroxidation are not higher in T cytoplasm than N cytoplasm anthers, it is unlikely that RF2A restores fertility to cmsT maize by oxidizing the products of lipid peroxidation.

IAA Biosynthesis

Because an ALDH from mung bean (*Vigna radiata*) seedlings can oxidize indole-3-acetaldehyde into IAA (Wightman and Cohen, 1968), it had been suggested that plant ALDHs may be involved in IAA biosynthesis (Marumo, 1986). There is, however, to date no evidence to either support or refute this physiological role for *rf2a*.

IAA can be synthesized from Trp, generating an indole-3-acetaldehyde intermediate, which can then be oxidized to form IAA (Normanly et al., 1995; Basse et al., 1996; Kawaguchi and Syono, 1996; Seo et al., 1998). The enzyme that catalyzes this oxidation has not yet been identified. Because RF2A has a K_m of 5.0 μM for indole-3-acetaldehyde, it is possible that RF2A could be involved in the production of IAA. However, because RF2A's K_{cat} for indole-3-acetaldehyde is low (8.2 s^{-1}), this would only occur in those cells in which RF2A accumulates to high levels.

Acetaldehyde

Another role that has been hypothesized for RF2A is the oxidation of acetaldehyde to acetate during ethanolic fermentation (Cui et al., 1996). Over the last several years, Cris Kuhlemeier's laboratory (Institute
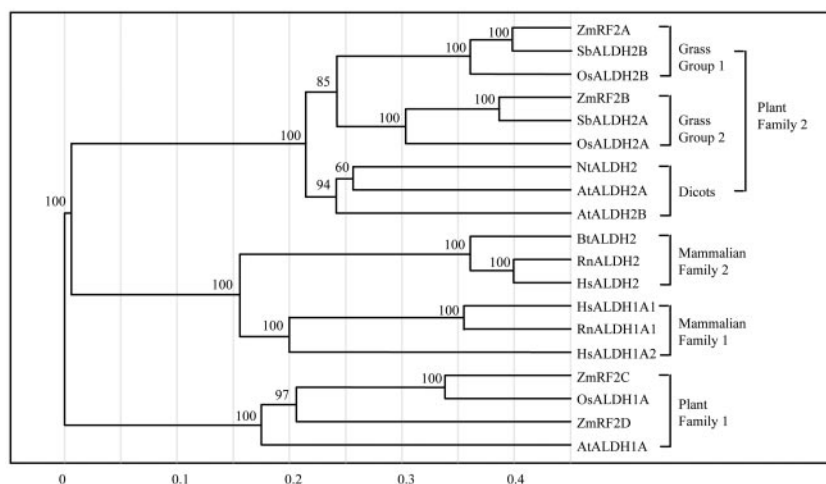
Figure 10. Phylogentic tree of plant and mammalian Family 1 and Family 2 ALDHs. Sequences were downloaded from GenBank or the Protein Data Bank and then aligned with ClustalX (Thompson et al., 1997); the tree was produced using the Genebee program (http://www.genebee.msu.su/services/phtree_reduced.html). Numbers shown at the branches of the tree are bootstrap values that indicate the percentage a particular branch was place at the position in 100 individual bootstrap experiments. The numbers shown below the frame indicate the proportion of amino acid changes. Zm, Maize; Sb, sorghum; Os, rice; Nt, tobacco; At, Arabidopsis; Bt, *Bos taurus*; Rn, *Rattus norvegicus*; Hs, human.

of Plant Physiology, University of Berne, Switzerland) has demonstrated that ethanolic fermentation occurs during pollen development and pollen germination (Tadege and Kuhlemeier, 1997; Tadege et al., 1999). Recently, his laboratory demonstrated that feeding germinating pollen with labeled ethanol results in the accumulation of label in CO_2 and lipids (Mellema et al., 2002). This is thought to occur via the serial action of ADH, ALDH, and acetyl-CoA synthase (EC 6.2.1.1). The kinetic analysis of RF2A is consistent with RF2A having a role in this pathway; RF2A's K_m for acetaldehyde is 2.4 μM and its K_{cat} is 100 s^{-1}. Hence, its K_{cat} to K_m ratio is 42, the highest ratio for all of the tested aldehydes. We conclude that RF2A can efficiently oxidize acetaldehyde. However, it is not yet possible to determine whether RF2A's acetaldehyde dehydrogenase activity is responsible for its role in fertility restoration and/or normal anther development.

Interestingly, RF2B oxidizes many fewer aldehydes than does RF2A and is more specific toward short-chain aliphatic aldehydes, including acetaldehyde. The *rf2b* mRNA accumulates to higher levels in plants that have been submerged, and these levels decrease after re-aeration (M. Nakazono, personal communication, unpublished data). In combination, these results suggest that RF2B may be primarily involved in ethanolic fermentation. In contrast, although RF2A can efficiently oxidize acetaldehyde, it is not induced by submergence (X. Cui and P.S. Schnable, unpublished data). Hence, it is unlikely that its major physiological role is resistance to anaerobic stress. *rf2a* mutants do not exhibit elevated sensitivity to anaerobic stress (X. Cui and P.S. Schnable, unpublished data). This provides another example of how RF2A and RF2B have undergone functional specialization.

RF2A May Function in Multiple Biochemical Pathways

Because most maize lines have never been exposed to T cytoplasm and yet carry functional alleles, we

have hypothesized that the RF2A protein has important functions other than restoration of cmsT (Schnable and Wise, 1994). The finding that RF2A is required for normal anther development in N cytoplasm maize established the validity of this hypothesis. Kinetic analyses of RF2A extend this conclusion. RF2A's broad substrate spectrum makes it a versatile enzyme that could potentially affect many cellular functions. For example, its capacity to oxidize benzaldehyde, anisaldehyde, glycolaldehyde, and cinnamaldehyde suggests that this enzyme could be involved in multiple pathways. Benzaldehyde is a precursor for some floral aromatic compounds (Dudareva and Pichersky, 2000); it is also involved in Phe metabolism (Nierop-Groot and de Bont, 1999). The aromatic compound anisaldehyde may be involved in plant-insect interactions (Teulon et al., 1993; Kubo and Kinst-Hori, 1998) and redox cycling of hydrogen peroxide (Guillen and Evans, 1994). Glycolaldehyde is a product of the degradation of carbohydrates (Voziyan et al., 2002) and a precursor of the glycolate pathway (Gambardella and Richardson, 1978); it is also an effective generator of free radicals (Hofmann et al., 1999). Cinnamaldehyde is involved in lignin biosynthesis (Kajita et al., 1996). Hence, based on its kinetic analyses and its expression in a wide variety of organs and at multiple developmental stages, it is possible that RF2A is involved in many biochemical pathways. However, because other enzymes accept some of these aldehydes as substrates, e.g. aldehyde oxidase (EC 1.1.1.21; Moriwaki et al., 2001), it is not yet possible to determine which aldehydes RF2A oxidizes in vivo.

Why Do Organisms Have Two mtALDHs?

In addition to maize, many other species have two mtALDH genes, including yeast (*Saccharomyces cerevisiae*; ALDH2 and ALDH5; Wang et al., 1998), human (ALDH2 and ALDH1B1), rice (ALDH2a and ALDH2b; Li et al., 2000), Arabidopsis (ALDH2a and ALDH2b; Li et al., 2000; Skibbe et al., 2002), and sorghum (ALDH2a

and ALDH2b; GenBank accession nos. AB084897 and AB084898). Because this genomic feature is conserved across taxa, including fungi, mammals, and plants, we hypothesize that this genomic feature has been maintained during evolution by selective pressure. This raises the question as to why mitochondria need two ALDHs. Mitochondria have different protein profiles at different developmental stages and/or in different organs (Wrutniak-Cabello et al., 2001). Hence, it is possible that the two mtALDHs are differentially expressed. In adult leaves, *rf2a* transcripts accumulate to higher levels than do *rf2b* transcripts (Fig. 3), and *rf2b*, but not *rf2a*, is induced by hypoxia.

However, we were also interested in testing the hypothesis that the two mtALDHs have different biochemical functions. To date, complete kinetic data have not been available for the two mtALDHs from any single organism. Although the kinetic features of the human mtALDH, ALDH2, have been well described (Greenfield and Pietruszko, 1977; Klyosov, 1996), kinetic data are not available for the other human mtALDH, ALDH1B1. In addition, kinetic data are not available for any purified plant mtALDH.

Here, we have reported the kinetic characterization of the two mtALDHs, RF2A and RF2B, from the model grass species, maize. RF2A is capable of oxidizing a wide range of aldehydes, whereas RF2B can oxidize only a few of the tested aldehydes. These two mtALDHs differ in other respects, such as their pH optima and their differential inhibition by substrates and disulfiram. In addition, RF2A, but not RF2B, exhibits positive cooperativity. These results demonstrate that the two mtALDHs of maize are likely to function in different biochemical pathways and under different physiological conditions.

Differential Accumulation of RF2A and RF2B in Tapetal Cells

Microspore abortion in cmsT maize is preceded by the premature degeneration of the innermost cell layer of anthers, the tapetal layer (Warmke and Lee, 1978). Previously, we have shown that RF2A antibodies cross-react with tapetal cells in Ky21 plants (Liu et al., 2001), a finding that is consistent with RF2A's role in complementing T cytoplasm-induced male sterility. In the absence of a mutant, it is not possible to determine whether a functional *rf2b* allele is required for normal anther development. However, data from the current study in combination with earlier data establish that RF2B protein does not accumulate to significant levels in tapetal cells. Previously, Liu et al. (2001) found that the tapetal cells of anthers that are homozygous for *rf2a-m8904* do not accumulate protein that reacts with the RF2A antibody. This means that either the RF2A antibodies do not detect RF2B or that RF2B does not accumulate in the tapetal cells. The finding that these antibodies cross-react with protein in root caps and seedling leaves of plants

homozygous for *rf2a-m8904* establishes that these antibodies detect RF2B. Hence, we conclude that RF2B does not accumulate to detectable levels in tapetal cells. This result provides further support that the two mtALDHs of maize have undergone functional specialization.

Structural Basis of the Kinetic Properties of RF2A and RF2B

Although RF2A and RF2B are about 83% similar, their substrate specificities and other kinetic characteristics are quite different. These differences must be a consequence of the differences in the sequences, i.e. the non-conserved amino acids must play important roles in the fine-tuning of the protein function. Based on predicted three-dimensional protein structures and phylogenic analyses, Pro-161/Thr-162, Tyr-162/Leu-163, Asp-395/Gly-396, Asp-296/Gly-297, and Asp-529/Tyr-530 may play roles in defining the differing kinetic properties of RF2A and RF2B. Because these residues are conserved within, but not between, the two mtALDHs clades of grasses, GGS1 and GGS2 (Fig. 9), we hypothesize that, like RF2A and RF2B, the pairs of mtALDHs from other grass species will also exhibit functional specialization.

MATERIALS AND METHODS

Plant Materials and Genotyping

The N cytoplasm version of the maize (*Zea mays*) inbred line Ky21 is homozygous for functional alleles of *rf2a* (RF2A-Ky21) and *rf2b* (RF2B-Ky21). This stock is maintained by self-pollination. The *rf2a-m8122* and *rf2a-m8904* alleles were backcrossed into N cytoplasm Ky21 for nine generations and then self-pollinated. Homogenous lines were established by self-pollinating homozygous individuals that had been identified via PCR-based genotyping (see below). The *rf2a-m8122* and *rf2a-m8904* alleles contain *Mu1* and *Ds1* transposon insertions, respectively, in their coding regions. The *Mu1* is located in exon 9 and the *Ds1* in exon 1 downstream from the initiation codon ATG (Cui et al., 2003).

Three pairs of PCR primers were used for identifying plants that were homozygous for *rf2a-m8122* or *rf2a-m8904*. The first primer pair, rf2a-4539 (5′-ACA TTG CCA TTA GCC CAG TG-3′) and rf2c14 (5′-GTG ATG GGC TCC TCT ACT G –3′), amplifies 0.8- and 0.45-kb PCR products from *Rf2a*-Ky21 and from *rf2a-m8904*, respectively. This primer pair does not amplify the *rf2a-8122* allele. The second primer pair, rf2c1 (5′-GCG TCG TTG GTG ATC CGT TC-3′) and Mu-TIR [5′-AGA GAA GCC AAC GCC A(AT) C GCC TC(CT) ATT TCG TC-3′] amplifies a 0.5-kb PCR product from *rf2a-m8122* and does not amplify *Rf2a*-Ky21. The third primer pair, Ds-8904 (5′-GGA TTC GGA AAC AAA TTC GG-3′) and rf2a-5UTRR (5′-CAT ATT TAT CCC GAT CCC CTT GAA-3′), amplifies a 0.7-kb PCR product from *rf2a-m8904* and does not amplify *Rf2a*-Ky21. All PCR reactions were carried out for 36 cycles (94°C, 35 s; 58°C, 35 s; and 72°C, 2.5 min).

Immunolocalization

Shoots and root tips from 5-d-old etiolated seedlings were cut into 0.2- to 0.5-cm segments and fixed in 4% (w/v) formaldehyde and 1% (v/v) glutaraldehyde in 50 mM PIPES buffer (pH 7.2) at 4°C overnight. These segments were dehydrated in a series of alcohol solutions (25%, 50%, 70%, 75%, 80%, 85%, 90%, 95%, 100% [twice; v/v], each for 2 h) and then infiltrated with ethanol:LR White resin (Electron Microscopy Sciences, Fort Washington, PA) in ratios of 1:3, 1:1, and 3:1 (v/v), and LR White resin (twice) for 12 h each (modified from Parthasarathy, 1994). The embedded sections were cross-sectioned (shoots) or longitudinal sectioned (root tips) into 1-μm-thick sections. Sections were then incubated at room temperature for 3 h with

affinity-purified anti-RF2A IgG (Liu et al., 2001) at 40 μg mL^{-1} concentration diluted in Tris-buffered saline (TBS) buffer containing 3% (w/v) bovine serum albumin, 3% (w/v) nonfat dry milk, and 1% (w/v) goat serum, and then incubated with 1:50 (v/v) diluted gold-labeled goat anti-rabbit IgG antibodies (Sigma, St. Louis) at room temperature for 2 h. The slides were washed with TBS and distilled water several times and then incubated with silver enhancer solution R-gent (Aurion, Wageningen, The Netherlands) for 20 min.

Purification of Recombinant RF2A and RF2B Proteins

Plasmids pMAP11 and pRB17 that express RF2A and RF2B, respectively, have been described previously (Liu et al., 2001; Skibbe et al., 2002). Because the coding regions of the respective cDNAs had been cloned into pET17b, protein expression, therefore, was under the control of the T$_7$ promoter in *Escherichia coli* strain BL21(DE3). Cells were cultured at 37°C until the optical density reached 0.7. Protein expression was then induced by the addition of 1 mM isopropylthio-β-galactoside and cultured at 30°C for an additional 5 to 6 h. Crude cell extracts were prepared as described previously (Liu et al., 2001) and loaded onto Whatman cellulose DE52 columns (2.5 × 20 cm), equilibrated with buffer A, which contained 25 mM HEPES (pH 7.4), 10% (v/v) glycerol, 1 mM dithiothreitol (DTT), and 1 mM EDTA. Columns were then washed with six volumes of the same buffer and eluted with 100 mM NaCl in buffer A. Three-milliliter fractions were collected and assayed for ALDH activity using 18 μM acetaldehyde as substrate as described by Liu et al. (2001). This assay is specific for recombinant ALDH because *E. coli* strain BL21(DE3) does not contain any endogenous acetaldehyde dehydrogenase activity that can be detected under these conditions (Liu et al., 2001). The pooled ALDH-containing fractions were passed through a Sephadex G-50 column (1.5 × 90 cm) equilibrated with phosphate-glycerol (PG) buffer (20 mM potassium phosphate buffer [pH 6.8], 10% [v/v] glycerol, and 1 mM DTT) at a rate of one drop every 20 s. ALDH-containing fractions were identified and pooled before being loaded onto a hydroxyapatite column equilibrated with PG buffer having an elevated phosphate concentration (80 mM). The column was washed with six volumes of PG buffer containing 80 mM potassium phosphate; ALDH was eluted with PG buffer containing 160 mM potassium phosphate. The pooled ALDH was then concentrated to 1 mL using an Ultra-free spin column (molecular weight cutoff 50, Millipore, Inc., Bedford, MA) and then diluted to 2 mL in phosphate-DTT (PD) buffer (40 mM potassium phosphate buffer [pH 6.4] and 1 mM DTT) before being loaded onto an NAD-agarose column (Sigma) equilibrated with PD buffer. The column was washed with PD buffer, and ALDH eluted with 0.1 M potassium phosphate (pH 7.6), 2.5 mM NAD, and 1 mM DTT. Glycerol was added to a final concentration of 25% (v/v) and the purified protein could be stored at −20°C for at least 15 months without losing activity.

The procedure used to purify RF2B was similar to that used to purify RF2A. The cellulose DE52 column was washed with 100 mM NaCl and RF2B protein was eluted with 130 mM NaCl. The hydroxyapatite column was washed with 20 mM potassium phosphate buffer (pH 6.8), 10% (v/v) glycerol, and 1 mM DTT, and RF2B was eluted with 50 mM potassium phosphate buffer (pH 6.8), 10% (w/v) glycerol, and 1 mM DTT. The pooled RF2B-containing fractions was then passed through a Blue-Cibracon GF-3A (Bio-Rad, Hercules, CA) column equilibrated with 20 mM potassium phosphate buffer (pH 6.8), 10% (v/v) glycerol, and 1 mM DTT and eluted with the same buffer. Glycerol was added to the final preparation to a final concentration of 25% (v/v).

In Vitro Import of RF2B Protein into Mitochondria

Plasmid pRBL1 was used for in vitro transcription/translation. PRBL1 was derived from pRB73 (Skibbe et al., 2002). Amplification of pRB73 with PCR primers rb7 (5′ TGC TAG CAA CCG TGA GGA GGG C 3′) and rbc9 (5′ CGG CGG TCT TGA GGA CGA CGG TGT T3′) resulted in the removal of the 5′-untranslated region from the *rf2b* cDNA. The resulting PCR product was digested with *Nhe*I and *Hin*dIII, and ligated into *Nhe*I/*Hin*dIII-digested pRB73 to generate pRBL1. The pRBL1 plasmid was linearized with *Eco*RV digestion and in vitro transcription/translation was carried out with the TNT quick transcription/translation kit from Promega (Madison, WI). Mitochondria were isolated from maize N cytoplasm Ky21 etiolated seedlings and purified via a three-step Percoll gradient centrifugation procedure (Jackson and Moore, 1979) and immediately used for import experiments. Import experiments were conducted according to Rudhe et al. (2002). SDS-

PAGE gels were dried in a frame sandwiched by two pieces of cellulosic microfiber membranes (BioDesign Gel wrap from BioDesign, Inc., Carmel, NY) and exposed at −70°C.

Determination of Molecular Masses of RF2A and RF2B

Purified recombinant RF2A and partially purified recombinant RF2B protein were used for molecular mass determinations on a Sephacryl S-300 column (1.5 × 90 cm) equilibrated with 20 mM sodium phosphate (pH 7.4), 0.1 M sodium chloride, 10% (v/v) glycerol, and 1 mM DTT. Carbonic anhydrase (29 kD), bovine albumin (66 kD), alcohol dehydrogenase (150 kD), β-amylase (200 kD), apoferritin (443 kD), and thyroglobulin (669 kD) were used as molecular mass standards (catalog no. MW-GF-1000, Sigma). Each protein was individually passed through the column at a constant flow rate of 25 s per drop. Fractions of 1.6 mL were collected. The presence of molecular mass standards in each fraction was monitored by A_{280}. RF2A and RF2B were individually passed through the column. The presence of RF2A and RF2B in fractions was monitored via an ALDH assay using 18 μM acetaldehyde as substrate. Void volumes (V_o) and elution volumes (V_e) of each protein were measured twice. Molecular masses were estimated via the semilog plot [Log(Mw) versus V_e/V_o] method (Marshall, 1970).

Enzyme Assays

ALDH assays were conducted as described previously (Liu et al., 2001). Esterase assays were performed according to Sheikh et al. (1997). The kinetics of RF2A were assayed in 0.1 M tetrasodium pyrophosphate buffer (pH 9.0) and 1.5 mM NAD$^+$. The kinetics of RF2B was assayed in 0.1 M sodium phosphate buffer (pH 7.5) and 1.5 mM NAD$^+$. All ALDH assays were conducted with a SpectroMax Gemini (Molecular Devices, Sunnyvale, CA) in a 96-well plate using a 300-μL reaction volume. Fluorescence of NADH was excited at 365 nm and emission at 460 nm was monitored. Kinetic parameters were calculated using the Enzfit program (Elsevier-Biosoft, Cambridge, UK). Inhibition of ALDH activity by disulfiram was measured as described by Lam et al. (1997). Before the ALDH assays were conducted, the purified RF2A or RF2B proteins were incubated with 0.5 mM disulfiram at room temperature for 15 min, respectively. The assay mixture contained 18 μM acetaldehyde and 1.5 mM NAD$^+$.

Formaldehyde, acetaldehyde, propionaldehyde, butyraldehyde, benzaldehyde, 4-nitrobenzaldehyde, *p*-anisaldehyde, and *m*-anisaldehyde were purchased from ACROS Organics/Fisher Scientific (Pittsburgh); valeraldehyde, hexanal, heptylaldehyde, octanal, nonanal, decanal, acrolein, trans-2-hexenal, trans-2-nonenal, citral, 9-cis-retinal, all-trans-retinal, chloroacetaldehyde, pyruvic aldehyde, and indole-3-acetaldehyde were purchased from Sigma; trans-cinnamaldehyde, *o*-nitrocinnamaldehyde, 2-naphthaldehyde, and indole-3-carboxyaldehyde were purchased from Aldrich (Milwaukee, WI); glycolaldehyde was purchased from ICN Biomedicals, Inc. (Aurora, OH); and 4-HNE was purchased from Calbiochem (San Diego).

To assay native mtALDH activity, mitochondria were purified from 7-d-old etiolated maize seedlings according to Jackson and Moore (1979). Mitochondrial pellets were resuspended in 50 mM HEPES (pH 7.4), 10% (v/v) glycerol, 0.25% (w/v) Triton X-100, 1 mM EDTA, and 1 mM DTT, and then sonicated using a Fisher Dismembrator (model F60). Disrupted mitochondria were centrifuged at 20,000g for 20 min and the supernatant used for ALDH assays. Each assay contained 1.2 mg of protein from the mitochondria extract and 1.5 mM NAD$^+$.

N-Terminal Sequencing of RF2A

Mitochondria were isolated from approximately 1 kg of 6-d-old etiolated seedlings from the N cytoplasm inbred Ky21 as described previously (Liu et al., 2001). A mitochondrial extract was prepared by sonicating mitochondria for 2 to 5 min in TBS buffer with 0.1% (w/v) Triton X-100 using a Fisher Dismembrator (model F60) followed by centrifugation at 12,000g for 20 min. The supernatant was then incubated with RF2A antisera protein A-agarose beads at room temperature for 30 min with gentle shaking. The agarose beads were spun down and washed three times with TBS, followed by a final wash in 10 mM Tris (pH 8.0). Gly-HCl (0.1 M, pH 2.8) was added to the beads that were then incubated at room temperature for 5 min. After

centrifugation at 2,000*g* for 5 min, the supernatant was collected and subjected to 10% (w/v) SDS-PAGE gel electrophoresis. Proteins were then transferred overnight to a PVDF membrane (Millipore, Inc.) using a Bio-Rad transfer device at 10 V. The PVDF membrane was stained with 0.05% (w/v) Coomassie Blue R-250 and destained with 45% (v/v) methanol and 10% (v/v) acetic acid. That portion of the membrane that contained the approximately 54-kD band was excised and washed with distilled water before being subjected to Edman degradation N-terminal sequencing at the Iowa State University Protein Facility (Ames).

RNA Gel Blotting

RNA samples were isolated according to the protocol posted at the Arabidopsis Functional Genomics Consortium Web site (http://www.Arabidopsis.org). All samples were collected from N cytoplasm Ky21 plants unless otherwise indicated. Seedling leaf and root RNAs were isolated from 7-d-old seedlings of N cytoplasm Ky21 or near-isogenic N cytoplasm seedlings homozygous for *rf2a-m8904*; husk, silk, and ear RNAs were isolated unpollinated ear shoots (approximately 10 cm in length); "young tassel" RNA was isolated from a tassel (approximately 15 cm in length) that was still deep in the leaf whorl and contained anthers that had not yet reached the middle microspore stage; "older tassel" RNA was isolated from a tassel that had already emerged from the leaf whorl but from which anthers (at the early microspore to late pollen stages) had not yet exerted. RNAs were electrophoresed through a formaldehyde-containing denaturing agarose gel (Sambrook et al., 1989) and then transferred to GeneScreen hybridization membranes (PerkinElmer, Boston). The *rf2a* transcripts were detected using as a probe a PCR product amplified from plasmid prf27311 (Cui et al., 1996) with primers rf2a5UTRF (5′-GCA CCG GCA GCC ATT ACT TAC T-3′) and rf2GE (5′-TGT ACG AGG GTC CAG AGT TG-3′). The *rf2b* transcripts were detected using as a probe a PCR product amplified from plasmid pRB73 (Skibbe et al., 2002) with primers rf2b5UTRF (5′-CTT TGT GGC GGC GAT GGT CA-3′) and rf2b5UTRR (5′-CAG CCC TCC TCA CGG TTG C-3′). Hybridizations were conducted at 68°C overnight (Sambrook et al., 1989).

RT-PCR

RNA from Ky21 or *rf2a-m8904* mutant plants was used as template for RT-PCR to amplify transcripts of *rf2a* (1 ng) or α-tubulin (10 ng). The primers for *rf2a* amplification were rf2ac7 (5′-CAA CTC TGG ACC CTC GTA CA-3′) and rf2a13-xq (5′-TAG CAA GAG CAG CAC CAG CAG-3′). The α-tubulin primers TB1 (5′-ATG GCA TCC AGG CTG ATG GT-3′) and TB2 (5′-TAT GGC TCA ACT ACC GAA GT-3′) were designed based on the cDNA sequence provided in GenBank accession number AF249276. RT-PCR was conducted using the One-Step RT-PCR kit (catalog no. 210212, Qiagen, Inc., Valencia, CA). First stand cDNA synthesis was conducted at 55°C for 30 min followed by 15 min at 95°C to activate the *Taq* DNA polymerase. The PCR reactions were then conducted for 30 cycles; each cycle included 94°C for 35 s, 58°C for 35 s, and 72°C for 2 min.

Three-Dimensional Protein Modeling

The structures of RF2A and RF2B were predicted by SWISS-MODEL (Guex and Peitsch, 1997) using known ALDH structures identified by the program. For both RF2A and RF2B, the templates were Protein Data Bank numbers 1A4S and 1BPW (cod betaine ALDH), 1A4Z and 1AG8 (bovine ALDH2), 1AD3 (rat ALDH3), 1BI9 (rat RALDH), 1BXS (sheep Class 1 ALDH), 1CW3 (human ALDH2), 1EYY and 1EZ0 (NADP⁺-dependent ALDH from *Vibrio harveyi*), and 1QI1, 1QI6, 1EUH, and 1QI1 (NADP⁺-dependent ALDH from *Streptococcus mutans*). Ribbon images were prepared using MOLMOL software (Koradi et al., 1996).

Assays of Lipid Peroxidation and ROS

Spikelets containing anthers from meiocyte to early microspore stages were ground in a homogenizing buffer containing 20 mM potassium phosphate (pH 7.0), 5 mM butylated hydroxytoluene, and 0.1% (w/v) trichloroacetic acid. The homogenate was passed through four layers of cheesecloth and centrifuged at 4,000*g* for 5 min. The supernatant was used to assay lipid peroxidation assay according to the manufacturer's instructions (catalog no.

FR12, Oxford Biomedical Research, Oxford, MI). Protein assays were conducted using a Bio-Rad protein assay kit.

Maize anthers from upper florets were dissected and immersed in 0.1 M potassium phosphate buffer (pH 7.0) containing 50 μM DCFDA (ACROS Organics) at room temperature for 20 min. After being washed three times in 0.1 M potassium phosphate buffer (pH 7.0), anthers were viewed under a fluorescence microscope (model SZX-ILLD100, Olympus, Tokyo) with an excitation wavelength of 488 nm and an emission wavelength of 515 nm.

LITERATURE CITED

Asker H, Davies DD (1985) Mitochondrial aldehyde dehydrogenase from plants. Phytochemistry **24**: 689–693

Balk J, Leaver CJ (2001) The PET1-CMS mitochondrial mutation in sunflower is associated with premature programmed cell death and cytochrome c release. Plant Cell **13**: 1803–1818

Basse CW, Lottspeich F, Steglich W, Kahmann R (1996) Two potential indole-3-acetaldehyde dehydrogenases in the phytopathogenic fungus *Ustilago maydis*. Eur J Biochem **242**: 648–656

Boronat A, Caballero E, Aguilar J (1983) Experimental evolution of a metabolic pathway for ethylene glycol utilization by *Escherichia coli*. J Bacteriol **153**: 134–139

Botsoglou NA, Fletouris DJ, Papageorgiou GE, Vassilopoulos VN, Mantis AJ, Trakatellis AG (1994) Rapid, sensitive, and specific thiobarbituric acid method for measuring lipid peroxidation in animal tissue, food, and feedstuff samples. J Agric Food Chem **42**: 1931–1937

Comporti M (1989) Three models of free radical-induced cell injury. Chem Biol Interact **72**: 1–56

Cui, X, Hsia A-P, Liu F, Ashlock D, Wise RP, Schnable PS (2003) Alternative transcription initiation sites and polyadenylation sites are recruited during *Mu* suppression at the *rf2a* locus of maize. Genetics (in press)

Cui X, Wise RP, Schnable PS (1996) The *rf2* nuclear restorer gene of male sterile T-cytoplasm maize. Science **272**: 1334–1336

Davies DD (1959) The purification and properties of glycolaldehyde dehydrogenase. J Exp Bot **11**: 289–295

Dudareva N, Pichersky E (2000) Biochemical and molecular genetic aspects of floral scents. Plant Physiol **122**: 627–633

Esterbauer H, Schaur RJ, Zollner H (1991) Chemistry and Biochemistry of 4-hydroxynonenal, malonaldehyde and related aldehydes. Free Radic Biol Med **11**: 81–128

Ferrandez A, Prieto MA, Garcia JL, Diaz E (1997) Molecular characterization of PadA, a phenylacetaldehyde dehydrogenase from *Escherichia coli*. FEBS Lett **406**: 23–27

Gamaley IA, Klyubin IV (1999) Roles of reactive oxygen species: signaling and regulation of cellular functions. Int Rev Cytol **188**: 203–255

Gambardella RL, Richardson KE (1978) The formation of oxalate from hydroxypyruvate, serine, glycolate and glyoxylate in the rat. Biochim Biophys Acta **544**: 315–328

Greenfield NJ, Pietruszko R (1977) Aldehyde dehydrogenases from human liver. Isolation via affinity chromatography and characterization of the isozymes. Biochim Biophys Acta **483**: 35–45

Guex N, Peitsch MC (1997) SWISS-MODEL and the Swiss-PdbViewer: an environment for comparative protein modeling. Electrophoresis **18**: 2714–2723

Guillen F, Evans CS (1994) Anisaldehyde and veratraldehyde acting as redox cycling agents for H₂O₂ production by *Pleurotus eryngii*. Appl Environ Microbiol **60**: 2811–2817

Hart GJ, Dickinson FM (1977) Some properties of aldehyde dehydrogenase from sheep liver mitochondria. Biochem J **163**: 261–267

Hind M, Corcoran J, Maden M (2002) Alveolar proliferation, retinoid synthesizing enzymes, and endogenous retinoids in the postnatal mouse lung. Different roles for Aldh-1 and Raldh-2. Am J Resp Cell Mol Biol **26**: 67–73

Hofmann T, Bors W, Stettmaier K (1999) Studies on radical intermediates in the early stage of the nonenzymatic browning reaction of carbohydrates and amino acids. J Agric Food Chem **47**: 379–390

Jansen GA, van den Brink DM, Ofman R, Draghici O, Dacremont G, Wanders RJ (2001) Identification of pristanal dehydrogenase activity in peroxisomes: conclusive evidence that the complete phytanic acid alpha-oxidation pathway is localized in peroxisomes. Biochem Biophys Res Commun **283**: 674–679

Jabs T (1999) Reactive oxygen intermediates as mediators of programmed cell death in plants and animals. Biochem Pharmacol **57**: 231–245

Kajita S, Katayama Y, Omori S (1996) Alterations in the biosynthesis of lignin in transgenic plants with chimeric genes for 4-coumarate:coenzyme A ligase. Plant Cell Physiol **37**: 957–965

Kawaguchi M, Syono K (1996) The excessive production of indole-3-acetic acid and its significance in studies of the biosynthesis of this regulator of plant growth and development. Plant Cell Physiol **37**: 1043–1048

Klyosov AA (1996) Kinetics and specificity of human liver aldehyde dehydrogenase toward aliphatic, aromatic, and fused polycyclic aldehydes. Biochemistry **35**: 4457–4467

Koradi R, Billeter M, Wüthrich K (1996) MOLMOL: a program for display and analysis of macromolecular structures. J Mol Graphics **14**: 51–55

Kubo I, Kinst-Hori I (1998) Tyrosinase inhibitors from anise oil. J Agric Food Chem **46**: 1268–1271

Lam JP, Mays DC, Lipsky JJ (1997) Inhibition of recombinant human mitochondrial and cytosolic aldehyde dehydrogenase by two candidates for the active metabolites of disulfiram. Biochemistry **36**: 13748–13754

Laughnan JR, Gabay-Laughnan S (1983) Cytoplasmic male sterility in maize (*Zea mays*). Annu Rev Genet **17**: 27–48

Li Y, Nakazono M, Tsutsumi N, Hirai A (2000) Molecular and cellular characterizations of a cDNA clone encoding a novel isozyme of aldehyde dehydrogenase from rice. Gene **249**: 67–74

Lindahl R, Petersen DR (1991) Lipid aldehyde oxidation as a physiological role for class 3 aldehyde dehydrogenases. Biochem Pharmacol **41**: 1583–1587

Liu F, Cui X, Horner HT, Weiner H, Schnable PS (2001) Mitochondrial aldehyde dehydrogenase activity is required for male fertility in maize. Plant Cell **13**: 1063–1078

Marshall JJ (1970) Comments on the use of blue dextran in gel chromatography. J Chromatogr **53**: 379–380

Marumo S (1986) Auxins. *In* N Takahashi, ed, Chemistry of Plant Hormones. CRC Press, Boca Raton, FL, pp 9–56

Meguro N, Nakazono M, Tsutsumi N, Hirai A (2001) Decreased transcription of a gene encoding putative mitochondrial aldehyde dehydrogenase in barley (*Hordeum vulgare* L.) under submerged conditions. Plant Biotechnol **18**: 223–228

Mellema S, Eichenberger W, Rawyler A, Suter M, Tadege M, Kuhlemeier C (2002) The ethanolic fermentation pathway supports respiration and lipid biosynthesis in tobacco pollen. Plant J **30**: 329–336

Møller IM (2001) A more general mechanism of cytoplasmic male fertility? Trends Plant Sci **6**: 560

Moriwaki Y, Yamamoto T, Takahashi S, Tsutsumi Z, Hada T (2001) Widespread cellular distribution of aldehyde oxidase in human tissues found by immunohistochemistry staining. Histol Histopathol **16**: 745–753

Morse D, Meighen E (1984) Detection of pheromone biosynthetic and degradative enzymes in vitro. J Biol Chem **259**: 475–480

Nakai K, Kanehisa M (1992) A knowledge base for predicting protein localization sites in eukaryotic cells. Genomics **14**: 897–911

Nakazono M, Tsuji H, Li Y, Saisho D, Arimura S, Tsutsumi N, Hirai A (2000) Expression of a gene encoding mitochondrial aldehyde dehydrogenase in rice increases under submerged conditions. Plant Physiol **124**: 587–598

Nierop-Groot MN, de Bont JAM (1999) Involvement of manganese in conversion of phenylalanine to benzaldehyde by lactic acid bacteria. Appl Environ Microbiol **65**: 5590–5593

Normanly J, Slovin JP, Cohen JD (1995) Rethinking auxin biosynthesis and metabolism. Plant Physiol **107**: 323–329

op den Camp RG, Kuhlemeier C (1997) Aldehyde dehydrogenase in tobacco pollen. Plant Mol Biol **35**: 355–365

Parthasarathy MV (1994) Transmission electron microscopy: chemical fixation, freezing methods, and immunolocalization. *In* M Freeling, V Walbot, eds, The Maize Handbook. Springer-Verlag, New York, pp 118–134

Peitsch MC, Schwede T, Guex N (2000) Automated protein modeling: the proteome in 3D. Pharmacogenomics **1**: 257–266

Perozich J, Nicholas H, Wang BC, Lindahl R, Hempel J (1999) Relationships within the aldehyde dehydrogenase extended family. Prot Sci **8**: 137–146

Royall JA, Ischiropoulos H (1993) Evaluation of 2′,7′-dichlorofluorescin and dihydrorhodamine 123 as fluorescent probes for intracellular H_2O_2 in cultured endothelial cells. Arch Biochem Biophys **302**: 348–355

Rudhe C, Chew O, Whelan J, Glaser E (2002) A novel in vitro system for simultaneous import of precursor proteins into mitochondria and chloroplasts. Plant J **30**: 1–9

Salvador A, Sousa J, Pinto RYE (2001) Hydroperoxyl, superoxide and pH gradients in the mitochondrial matrix: a theoretical assessment. Free Radic Biol Med **31**: 1208–1215

Sambrook J, Fritsch EF, Maniatis T (1989) Molecular Cloning: A Laboratory Manual, Ed 2. Cold Spring Harbor Laboratory Press, Cold Spring Harbor, NY

Satomichi A, Nakajima Y, Takeuchi A, Takagaki Y, Saigenji K, Shibuya A (2000) Primary structure of human hepatocellular carcinoma-associated aldehyde dehydrogenase. Biochim Biophys Acta **1481**: 328–336

Schnable PS, Wise RP (1994) Recovery of heritable, transposon-induced, mutant alleles of the *rf2* nuclear restorer of T-cytoplasm maize. Genetics **136**: 1171–1185

Schnable PS, Wise RP (1998) The molecular basis of cytoplasmic male sterility and fertility restoration. Trends Plant Sci **3**: 175–180

Seo M, Akaba S, Oritani T, Delarue M, Bellini C, Caboche M, Koshiba T (1998) Higher activity of an aldehyde oxidase in the auxin-overproducing superroot1 mutant of *Arabidopsis thaliana*. Plant Physiol **116**: 687–693

Sheikh S, Ni L, Hurley TD, Weiner H (1997) The potential roles of the conserved amino acids in human liver mitochondrial aldehyde dehydrogenase. J Biol Chem **272**: 18817–18822

Sidhu RS, Blair AH (1975) Human liver aldehyde dehydrogenase: kinetics of aldehyde oxidation. J Biol Chem **250**: 7899–7904

Sjöling S, Glaser E (1998) Mitochondrial targeting peptides in plants. Trends Plant Sci **3**: 136–140

Skibbe DS, Liu F, Wen TJ, Yandeau MD, Cui X, Cao J, Simmons CR, Schnable PS (2002) Characterization of the aldehyde dehydrogenase gene families of *Zea mays* and Arabidopsis. Plant Mol Biol **48**: 751–764

Sladek NE (1988) Metabolism of oxazaphosphorines. Pharmacol Ther **37**: 301–355

Sophos NA, Pappa A, Ziegler TL, Vasiliou V (2001) Aldehyde dehydrogenase gene superfamily: the 2000 update. Chem Biol Interact **130–132**: 323–337

Steinmetz CG, Xie P, Weiner H, Hurley TD (1997) Structure of mitochondrial aldehyde dehydrogenase: the genetic component of ethanol aversion. Structure **5**: 701–711

Styrvold OB, Falkenberg P, Landfald B, Eshoo MW, Bjrnsen T, Strom AR (1986) Selection, mapping, and characterization of osmoregulatory mutants of *Escherichia coli* blocked in the choline-glycine betaine pathway. J Bacteriol **165**: 856–863

Tadege M, Dupuis I, Kuhlemeier C (1999) Ethanolic fermentation: new function for an old pathway. Trends Plant Sci **4**: 320–325

Tadege M, Kuhlemeier C (1997) Aerobic fermentation during tobacco pollen development. Plant Mol Biol **35**: 343–354

Tamaki N, Kimura K, Hama T (1978) Studies on the oligomeric structure of yeast aldehyde dehydrogenase by cross-linking with bifunctional reagents. J Biochem **83**: 21–25

Teulon DAJ, Penman DR, Ramakers PMJ (1993) Volatile chemicals for thrips (Thysanoptera: Thripidae) host-finding and applications for thrips pest management. J Econ Entomol **86**: 1405–1415

Thompson JD, Gibson TJ, Plewniak F, Jeanmougin F, Higgins DG (1997) The ClustalX windows interface: flexible strategies for multiple sequence alignment aided by quality analysis tools. Nucleic Acids Res **24**: 4876–4882

Voziyan PA, Metz TO, Baynes JW, Hudson BG (2002) A post-Amadori inhibitor pyridoxamine also inhibits chemical modification of proteins by scavenging carbonyl intermediates of carbohydrate and lipid degradation. J Biol Chem **277**: 3397–3403

Wang X, Mann CJ, Bai Y, Ni L, Weiner H (1998) Molecular cloning, characterization, and potential roles of cytosolic and mitochondrial aldehyde dehydrogenases in ethanol metabolism in *Saccharomyces cerevisiae*. J Bacteriol **180:** 822–830

Warmke HE, Lee SLJ (1978) Pollen abortion in T cytoplasmic male-sterile corn (*Zea mays*): a suggested mechanism. Science **200:** 561–563

Weiner H, Hu JH, Sanny CG (1976) Rate-limiting steps for the esterase and dehydrogenase reaction catalyzed by horse liver aldehyde dehydrogenase. J Biol Chem **251:** 3853–3855

Wightman F, Cohen D (1968) Intermediary steps in the enzymatic conversion of tryptophan to IAA in cell-free systems from mung bean seedlings. *In* F Wightman, G Setterfield, eds, Biochemistry and Physiology of Plant Growth Substances: Proceedings of the 6th International Conference on Plant Growth Substances. Runge Press, Ottawa, Canada, p 273

Winning BM, Sarah CJ, Leaver CJ (1995) Protein import into plant mitochondria. Methods Enzymol **260:** 293–302

Wrutniak-Cabello C, Casas F, Cabello G (2001) Thyroid hormone action in mitochondria. J Mol Endocrinol **26:** 67–77